APPLIED PHYSICS LETTERS **104**, 033106 (2014)

Morphology evolution in strain-compensated multiple quantum well structures

N. N. Ledentsov,[1,a)] V. A. Shchukin,[1] and S. Rouvimov[2]
[1]*VI Systems GmbH, Hardenbergstraße 7, Berlin D-10623, Germany and A. F. Ioffe Physical Technical Institute of the Russian Academy of Sciences, Politekhnicheskaya 26, St. Petersburg 194021, Russia*
[2]*University of Notre Dame, 112 North Notre Dame Avenue, South Bend, Indiana 46556, USA*

(Received 14 November 2013; accepted 5 January 2014; published online 23 January 2014)

Morphology evolution in (In,Ga)As-Ga(As,P) strain-compensated multilayer structures is studied. The effects of nanoscale interface corrugation and phase separation are evident after the third period of the multilayer structure and become more pronounced with each new stack until the sixth period. Then, the interface stabilizes pointing to the formation of strain-balanced equilibrium interface structure. The epitaxial structure remains defect-free up to the maximum number (twenty) of periods studied. In a structure with a high lattice mismatch between the neighboring layers, $In_{0.40}Ga_{0.60}As/GaAs_{0.85}P_{0.15}$, clusters of dislocations are revealed already in the third period. The observed phenomena are critical for proper engineering of optoelectronic devices. © *2014 AIP Publishing LLC*. [http://dx.doi.org/10.1063/1.4862436]

Multiple stacks of strain-compensated quantum wells (QWs) (e.g., (In,Ga)As-Ga(As,P) structures) are widely used in optoelectronic devices, e.g., in light-emitting or laser diodes, photodetectors, solar cells, etc. Of particular interest are high power high-brightness laser diodes in which a thick vertical waveguide is applied[1–8] suppressing catastrophic optical mirror damage, beam filamentation, thermal "smile" of a laser bar, what is of high importance for wavelength stabilization of the bars by external diffraction gratings.[3] Optical losses < 0.4 cm^{-1} were reported for thick waveguide laser diodes with vertical beam divergence $\sim 30°$ (full width at half maximum, FWHM).[1] To advance the concept to even thicker waveguides, multiple QWs (MQWs) must be used to counteract the reduced optical confinement factor.[2,3,5,7,8] To keep the gain region compact allowing the vertical mode selection,[1,2] on the one hand, and for avoiding defect formation in stacked InGaAs QWs,[6] on the other hand, strain compensation by GaAsP barriers is usually applied. Vertical beam divergences of only 8° (Ref. 2), $\sim 5°$ (Ref. 7), and $\sim 0.7°$ (Refs. 4 and 5) were realized. It was noted, however, that laser diodes with GaAsP strain compensation barriers demonstrate higher waveguide losses and thus lower wall-plug efficiencies as compared to the lasers with stacked QWs grown without strain-compensation.[9] Furthermore, ultranarrow beam QW lasers (FWHM $< 0.7°$) so far demonstrated only moderate differential efficiency at long cavity lengths (50%, $L = 3.5$ mm, as cleaved facets).[5] It was noted, on the other hand, that very small concentrations of Phosphorus improve laser performance.[10] Thus, there is a need to understand the reason of the discrepancies reported in multiple research publications.

The origin of increased waveguide losses may be related to the sensitivity of the intensity mode profile to minor changes of the refractive index within the waveguide in thick waveguide structures. Thus, local inhomogeneities of the refractive index in the MQW region may be critical for the performance of the device.[2]

It should be noted that compositional and morphological inhomogeneities in the alloy growth are inherently connected.[11,12] Laterally modulated structures occur also at the growth of alloy films lattice-matched to the substrate.[13,14] A larger variety of instabilities and related modulated structures occur at the growth of multilayer films,[15] both without and with strain compensation. Theoretical papers[16–18] emphasize that the strain profile at the surface of a growing crystal governing the morphology evolution is created by the buried undulated interfaces and therefore strongly depends on the layer thickness. The strain changes its sign upon the layer thickness providing a transition from the out-of-phase morphological instability (regarding subsequent interfaces) to stable growth and further to in-phase instability. As the strain created by the interface undulations decays exponentially with the distance, only a small number of buried interfaces contribute to the strain at the surface. That is why, one may expect that the (in)stability criteria will be different for a few first layers, on the one hand, and for higher layers, on the other hand.

In this Letter, we study the structural properties of multiple InGaAs-GaAsP layer stacks and show that both layer thickness and composition can be significantly modulated already in the third period. Furthermore, above a critical difference in compositions between neighboring layers, dislocated clusters appear in the third period.

The structures were grown by metal-organic chemical vapor deposition on (100)GaAs semi-insulating substrates using trimethylindium, trimethylgallium, arsine, and phosphine. A 300 nm-thick GaAs buffer layer was deposited at 650 °C followed by a 10 nm-thick $Al_{0.3}Ga_{0.7}As$ and a 20 nm-thick GaAs layer. Then, the temperature was reduced to 600 °C, and a 15 nm-thick $GaAs_{0.87}P_{0.13}$ tensile strained barrier layer was deposited, followed by a 7 nm-thick compressively strained $In_{0.24}Ga_{0.76}As$ with a narrow bandgap and then by another 15 nm-thick $GaAs_{0.87}P_{0.13}$ barrier layer.

[a)]Electronic mail: nikolay.ledentsov@v-i-systems.com

 © 2014 AIP Publishing LLC

The number of stacks varied between 2 and 20. The photoluminescence (PL) emission at room temperature was at 1035–1040 nm with the FWHM ~ 22–26 nm, weakly dependent on the number of stacks. The structure was capped by a 10 nm-thick GaAs layer, $Al_{0.3}Ga_{0.7}As$ layer and a 5 nm-thick GaAs cap layer. In another growth run, both the Indium composition in the QWs and the Phosphorus composition in the barriers were increased ($In_{0.40}Ga_{0.60}As$ and $GaAs_{0.85}P_{0.15}$). The substrate temperature during the active region deposition was reduced to about 550 °C.

Structural properties of multilayer systems were studied by transmission electron microscopy (TEM). A FEI Titan 80–300 TEM was used for high resolution transmission electron microscopy (HRTEM) and high resolution scanning transmission electron microscopy (HR STEM) imaging and compositional analysis.[19] The high angle annular dark field (HAADF) images in STEM mode provide direct visualization of compositional variations at atomic resolution due to the sensitivity of the HAADF contrast to the atomic number (Z-contrast).[19] In addition, (002) dark-field TEM images sensitive to structure factor difference between group-III and group-V elements[20] were used to observe the composition variations. Compositional analysis was performed by energy dispersive X-ray spectroscopy (EDS). Cross-sectional TEM specimens were prepared by Focus Ion Beam (FIB) technique on FEI Helios Nano-Lab Dual Beam 600 SEM/FIB Workstation.

The TEM images of the 20-layer structure with a lower Indium composition in the strain-sensitive conditions is shown in Fig. 1, where thinner layers are (In,Ga)As regions and thicker layers refer to Ga(As,P) regions. Corrugation and strain nonuniformities increase with the layer's number, and (In,Ga)As insertions in the top part of Fig. 1 are no longer planar layers. Furthermore, the formation of well resolved quantum dot-like structures aligned in tilted directions[21] is clearly observable.

As the strain contrast may interfere with composition-induced features, structural analysis in chemically-sensitive conditions is desirable. In the HAADF STEM image (Fig. 2) of the same 20-fold stacked strain-compensated structure, bright areas are Indium-rich (InGaAs), dark areas are

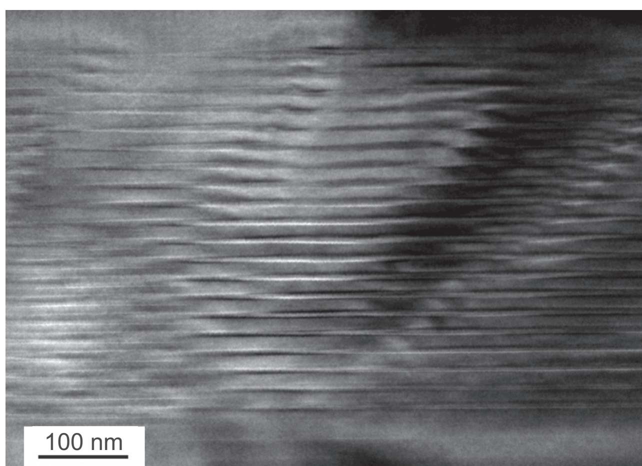

FIG. 1. Transmission electron microscopy image of the $GaAs_{0.87}P_{0.13}$-$In_{0.24}Ga_{0.76}As$ multilayer structure taken in strain-sensitive conditions.

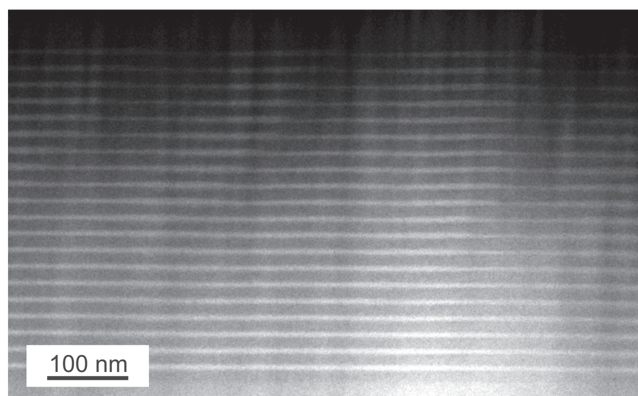

FIG. 2. The high angle annular dark field image in scanning transmission electron microscopy mode of the $GaAs_{0.87}P_{0.13}$-$In_{0.24}Ga_{0.76}As$ multilayer structure.

Phosphorus-rich (GaAsP), while GaAs refers to an intermediate gray contrast.

In Fig. 2, the bottom layers show reasonable uniformity, stacking results in the evolution of well-defined Indium-rich domains, either vertically aligned or tilted. Phosphorus-rich domains are vertically aligned. Even the average contrast changes with darkening of the image towards the top, one may conclude that the modulation strength of the InGaAs layers reaches maximum by the 10th−11th period and then stabilizes.

As regards structural defects, one should note that a foil for TEM studies is typically 10–20 nm-thick, and a probability to observe a defect cluster is relatively low for moderate defect densities. In our study, multiple cross sectional TEM images at low magnification (with a lateral dimension of the area ~5 μm) were aligned to ensure no defects over at least 100 μm distance.

To estimate the degree of compositional modulation, the EDS line scans were constructed from the integrated regions corresponding to the elemental peaks in the X-ray spectrum (see, e.g., Refs. 22 and 23). The data on EDS scans in the direction perpendicular to the layer planes are presented in Fig. 3. The resolution of the technique is high and reveals that the chemical compositions of all key elements show clear correlations or anti-correlations. The Galium peak intensity decreases while the Indium peak intensity increases within the InGaAs layers. The Arsenic peak intensity decreases in GaAsP regions in anti-correlation with the Phosphorus peak intensity.

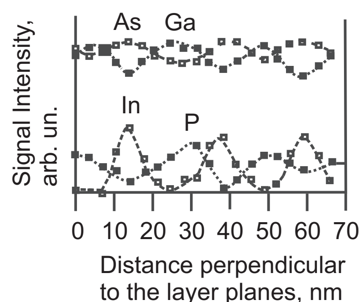

FIG. 3. Energy dispersive X-ray spectroscopy line scans in the direction perpendicular to the layer planes.

In Fig. 4, EDS line scans in the direction parallel to the layer planes for different periods and layer types are shown. In this case, no intensity modulation is expected for planar layers. However, as the scanning direction is not ideally parallel to the layer planes, smooth transition regions at significant scanning lengths may appear. Such a trend is revealed basically in the first period. A smooth variation of the Indium composition is observed. Phosphorus composition is low in the InGaAs regions while Indium composition is low in the GaAsP regions. The situation changes remarkably already for the third period, where significant compositional modulations occur. Furthermore, the contribution of the Phosphorus and Indium peak intensities increases in the InGaAs and GaAsP regions, respectfully. In higher stacking periods, a further dramatic change happens. The composition modulation amplitude increases drastically exceeding 50% for Indium and Phosphorus in the related areas. Anti-correlation of Indium and Phosphorus peak intensities is broken and significant peak intensities for both elements coexist in the same areas. This may indicate that the morphology evolution is significant and that InGaAs layers do not fully cover the modulated GaAsP surface resulting in areas with strong intermixing of Indium and Phosphorus.

The characteristic periodicities of the modulation may reach 60–100 nm or about 1/3 to 1/4 of the wavelength in the crystal at ∼1000 nm. Thus, a significant light scattering loss may be expected in multi-stacked strain compensated QW

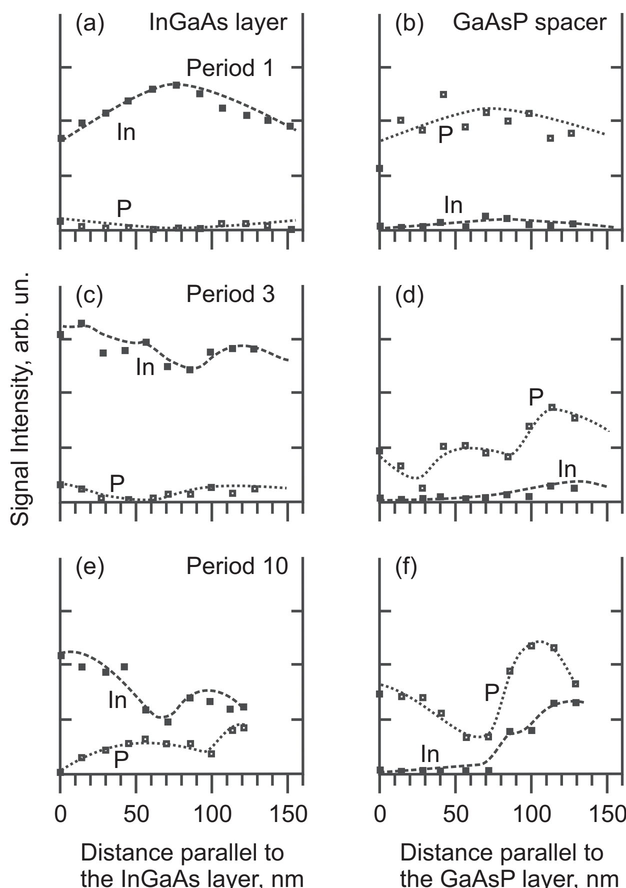

FIG. 4. Energy dispersive X-ray spectroscopy line scans in the direction parallel to the layer planes for the first ((a) and (b)), third ((c) and (d) and tenth ((e) and (f)) periods for InGaAs ((a)–(c)) and GaAsP ((b)–(f)) regions of the strain-compensated structure.

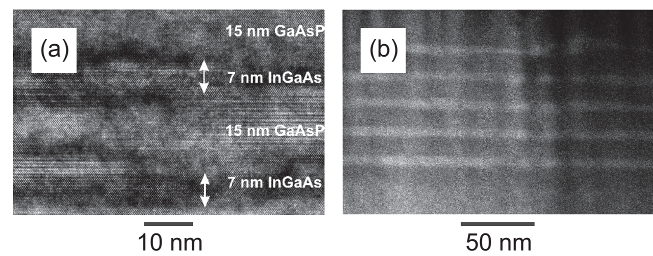

FIG. 5. High resolution transmission electron microscopy (a) and high angle annular dark field scanning transmission electron microscopy (b) images of the $GaAs_{0.85}P_{0.15}$-$In_{0.40}Ga_{0.60}As$ multilayer structure.

structures used in thick waveguide lasers. As opposite, the structures with one or two stacks (below 3) should not suffer from such phenomenon. The fact that stacking-induced morphology evolution stabilizes after about 6th–10th period and does not result in formation of defects allows extension of the absorption edge if multiple closely stacked layers are used in solar cells and top-illuminated photodetectors.

Further, the impact of the absolute strain in the InGaAs and GaAsP regions on the morphology evolution in multi-stack structures is studied. Figures 5(a) and 5(b) show the HRTEM and HAADF STEM images of the $In_{0.40}Ga_{0.60}As/GaAs_{0.85}P_{0.15}$ multilayer structure emitting at 1.18 μm. One can see in Fig. 5(a) that even the interfaces in the HRTEM image for the first period are planar, further interfaces are poorly resolved. Also for the first interface, local irregularities can be observed. The chemically-sensitive image of Fig. 5(b) reveals, opposite to the case of Fig. 2, compositional modulations already clearly visible in the first periods, due to a higher Indium and Phosphorus content in individual layers. Thus, the related light scattering may become important also for single strain-compensated QW lasers with high Indium composition emitting at 1220 nm.[6] Another observation is a much smaller lateral periodicity of the lateral compositional modulation of 20–40 nm instead of 100–400 nm revealed in Fig. 2 for the same period numbers.

It should also be noted that the strain compensated structures with larger relative strain exhibit local formation of heavily dislocated clusters, as shown in Fig. 6. The defects are found to originate in the third period of the multilayer stack, while the bottom periods are defect-free. Bending of the surface on a lateral scale of 200–300 nm is revealed on top of the structure. We attribute this effect to the defect-induced accumulation of critical local strain triggering the morphology evolution. The rest of the structure remains coherent to the substrate.

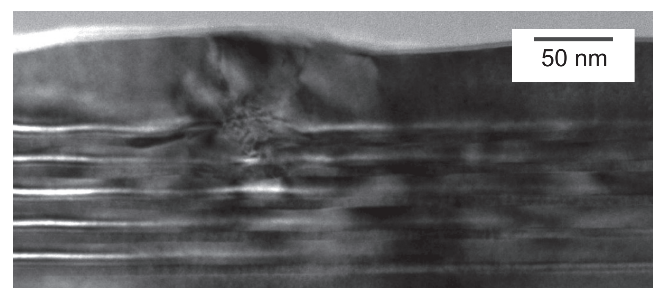

FIG. 6. Transmission electron microscopy image of the $GaAs_{0.85}P_{0.15}$-$In_{0.40}Ga_{0.60}As$ multilayer structure taken in strain-sensitive conditions.

To conclude, we studied structural properties of strain-compensated (InGa)As-Ga(As,P) multilayer structures. We observed a strong compositional modulation for the structures with significant relative lattice mismatch between the layers. Defect formation is revealed in the upper periods in this case. Even the observations are performed for (In,Ga)As-Ga(As,P) multilayer stacks, general conclusions may be applied to other combinations of III-V, III-N, and II-VI materials.

The work was supported by the EU FP7 program under Agreement No. 318338 and the PIANO+ Collaborative R&D program (project SEPIANet).

[1] D. A. Vinokurov, S. A. Zorina, V. A. Kapitonov, A. V. Murashova, D. N. Nikolaev, A. L. Stankevich, M. A. Khomylev, V. V. Shamakhov, A. Yu. Leshko, A. V. Lyutetskii, T. A. Nalyot, N. A. Pikhtin, S. O. Slipchenko, Z. N. Sokolova, N. V. Fetisova, and I. S. Tarasov, Semiconductors **39**, 370 (2005).

[2] A. Pietrzak, P. Crump, H. Wenzel, G. Erbert, F. Bugge, and G. Tränkle, IEEE J. Sel. Top. Quantum Electron. **17**, 1715 (2011).

[3] P. Crump, S. Knigge, A. Maaßdorf, F. Bugge, S. Hengesbach, U. Witte, H.-D. Hoffmann, B. Köhler, R. Hubrich, H. Kissel, J. Biesenbach, G. Erbert, and G. Traenkle, Proc. SPIE **8605**, 86050T (2013).

[4] V. Shchukin, N. Ledentsov, K. Posilovic, V. Kalosha, Th. Kettler, D. Seidlitz, M. Winterfeldt, D. Bimberg, N. Yu. Gordeev, L. Ya. Karachinsky, I. I. Novikov, Yu. M. Shernyakov, A. V. Chunareva, M. V. Maximov, F. Bugge, and M. Weyers, IEEE J. Quantum Electron. **47**, 1014 (2011).

[5] N. N. Ledentsov, V. A. Shchukin, I. I. Novikov, N. Yu. Gordeev, M. V. Maximov, Yu. M. Shernyakov, A. S. Pausov, K. Posilovic, T. Kettler, D. Bimberg, F. Bugge, and M. Weyers, Electron. Lett. **47**, 1339 (2011).

[6] D. A. Vinokurov, V. A. Kapitonov, D. N. Nikolaev, N. A. Pikhtin, A. L. Stankevich, V. V. Shamakhov, A. D. Bondarev, L. S. Vavilova, and I. S. Tarasov, Semiconductors **45**, 1364 (2011).

[7] I. I. Novikov, N. Yu. Gordeev, Yu. M. Shernyakov, Yu. Yu. Kiselev, M. V. Maximov, P. S. Kop'ev, A. Sharon, R. Duboc, D. B. Arbiv, U. Ben-Ami, V. A. Shchukin, and N. N. Ledentsov, Appl. Phys. Lett. **92**, 103515 (2008).

[8] M. V. Maximov, Yu. M. Shernyakov, I. I. Novikov, L. Ya. Karachinsky, N. Yu. Gordeev, U. Ben-Ami, D. B. Arbiv, A. Sharon, V. A. Shchukin, N. N. Ledentsov, T. Kettler, K. Posilovic, and D. Bimberg, IEEE J. Sel. Top. Quantum Electron. **14**, 1113 (2008).

[9] F. Bugge, U. Zeimer, H. Wenzel, R. Staske, B. Sumpf, G. Erbert, M. Weyers, and G. Tränkle, Phys. Status Solidi C **3**, 423 (2006).

[10] D. A. Vinokurov, A. V. Lyutetskiy, D. N. Nikolaev, V. V. Shamakhov, K. V. Bakhvalov, V. V. Vasylyeva, L. S. Vavilova, M. G. Rastegaeva, and I. S. Tarasov, Semiconductors **47**, 1075 (2013).

[11] B. J. Spencer, P. W. Voorhees, and J. Tersoff, Phys. Rev. Lett. **84**, 2449 (2000).

[12] Zh.-F. Huang and R. C. Desai, Phys. Rev. B **65**, 205419 (2002).

[13] S. W. Jun, T.-Y. Seong, J. H. Lee, and B. Lee, Appl. Phys. Lett. **68**, 3443 (1996).

[14] Q. Y. Wei, T. Li, Y. Huang, J. Y. Huang, Z. T. Chen, T. Egawa, and F. A. Ponce, Appl. Phys. Lett. **100**, 092101 (2012).

[15] A. G. Norman, S. P. Ahrenkiel, H. Moutinho, M. M. Al-Jassim, A. Mascarenhas, J. Mirecki Millunchick, S. R. Lee, R. D. Twesten, D. M. Follstaedt, J. L. Reno, and E. D. Jones, Appl. Phys. Lett. **73**, 1844 (1998).

[16] L. E. Shilkrot, D. J. Srolovitz, and J. Tersoff, Phys. Rev. B **62**, 8397 (2000); **67**, 249901(E) (2003).

[17] Zh. -F. Huang and R. C. Desai, Phys. Rev. B **67**, 075416 (2003).

[18] Zh. -F. Huang, D. Kandel, and R. C. Desai, Appl. Phys. Lett. **82**, 4705 (2003).

[19] D. Williams and C. B. Carter, *Transmission Electron Microscopy: A Textbook for Materials Science* (Springer, Berlin, 1996).

[20] R. Beanland, Ultramicroscopy **102**, 115 (2005).

[21] V. A. Shchukin, N. N. Ledentsov, and D. Bimberg, *Epitaxy of Nanostructures* (Springer, Berlin, 2003).

[22] A. J. D'Alfonso, B. Freitag, D. Klenov, and L. J. Allen, Phys. Rev. B **81**, 100101 (2010).

[23] V. Shchukin, N. Ledentsov, and S. Rouvimov, Phys. Rev. Lett. **110**, 176101 (2013).